This is an open access article published under an ACS AuthorChoice License, which permits copying and redistribution of the article or any adaptations for non-commercial purposes.

ACS OMEGA

Article

Cite This: ACS Omega 2017, 2, 9144−9149

Nanosized Gadolinium and Uranium—Two Representatives of High-Reactivity Lanthanide and Actinide Metal Nanoparticles

Christian Schöttle,[†] Stefan Rudel,[‡] Radian Popescu,[§] Dagmar Gerthsen,[§] Florian Kraus,*[,‡] and Claus Feldmann*[,†]

[†]Institut für Anorganische Chemie, Karlsruhe Institute of Technology (KIT), Engesserstraße 15, 76131 Karlsruhe, Germany

[‡]Fachbereich Chemie, University of Marburg, Hans-Meerwein-Straße 4, 35032 Marburg, Germany

[§]Laboratorium für Elektronenmikroskopie, Karlsruhe Institute of Technology (KIT), Engesserstraße 7, 76131 Karlsruhe, Germany

Supporting Information

ABSTRACT: Gadolinium (Gd^0) and uranium (U^0) nanoparticles are prepared via lithium naphthalenide ([LiNaph])-driven reduction in tetrahydrofuran (THF) using $GdCl_3$ and UCl_4, respectively, as low-cost starting materials. The as-prepared Gd^0 and U^0 suspensions are colloidally stable and contain metal nanoparticles with diameters of 2.5 ± 0.7 nm (Gd^0) and 2.0 ± 0.5 nm (U^0). Whereas THF suspensions are chemically stable under inert conditions (Ar and vacuum), nanoparticulate powder samples show high reactivity in contact with, for example, oxygen, moisture, alcohols, or halogens. Such small and highly reactive Gd^0 and U^0 nanoparticles are first prepared via a dependable liquid-phase synthesis and stand as representatives for further nanosized lanthanides and actinides.

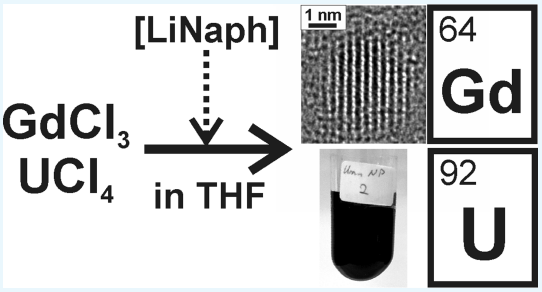

INTRODUCTION

The access to metal nanoparticles is the more challenging the lower the electrochemical potential of the metal, and the smaller the size of the particles.[1] Both—strong base character and small size—result in a tremendous increase of the nanoparticle reactivity. In this context, iron is an illustrative example: whereas the corrosion of bulk iron occurs on a timescale of several months and years, nanosized iron is pyrophoric and shows immediate ignition in contact with air.[2] This enormous increase in reactivity is related to the significantly higher surface area and the absence of any passivation layer.[1] In terms of standard electrode potential, however, bulk iron ($E_0^{bulk}(Fe^0/Fe^{3+})$ = −0.81 V) still has a moderate base character.[3] The realization of nanosized lanthanide and actinide metals is another magnitude of challenge that is addressed here with gadolinium ($E_0^{bulk}(Gd^0/Gd^{3+})$ = −2.28 V)[3] and uranium ($E_0^{bulk}(U^0/U^{4+})$ = −2.23 V)[3] nanoparticles as representative examples. Although the standard electrode potentials (taken for alkaline conditions) account for high oxygen affinity and high chemical reactivity of gadolinium and uranium, they only refer to the bulk metals. Nanosized Gd^0 and U^0 are of course much more reactive as implied by the standard electrode potential of the bulk metals.

Nanoparticles of highly reactive base metals are yet most often made via gas-phase techniques or by the decomposition of elaborate metal−organic precursors, partially involving harsh and less reproducible conditions.[4−6] In view of Gd^0 and U^0, only few publications are available and involve evaporation methods, γ-ray irradiation, and pulsed laser ablation.[7−9] These methods only result in nonuniform, heavily aggregated, and partially oxidized particles. In this concern, it needs to be noted that the most nanoparticles designated "gadolinium" or "gadolinium-based" contain only Gd^{3+} (e.g., Gd_2O_3).[10−14] The only option for the liquid-phase synthesis of Gd^0 nanoparticles dates back to Tsai and Dye and the use of crown ether-stabilized alkalides as powerful reducing agents.[15] This strategy was developed further by Wagner et al., who studied the magnetic properties in detail.[16] Via electron microscopy, however, they could only identify 10−15 nm sized Gd_2O_3 nanoparticles. Recently, they also prepared Gd@Au core−shell nanoparticles comprising a dense gold shell to protect the Gd^0 core from oxidation.[17] In regard to U^0—to the best of our knowledge—not any liquid-phase synthesis of nanoparticles has been reported yet.

Taken together, straightforward liquid-phase synthesis of Gd^0 and U^0 nanoparticles is lacking. Dependable and comparably simple synthesis is even more relevant because Gd^0 and U^0 stand as representatives for further lanthanide and actinide metals. Owing to this concern, we present here the synthesis of Gd^0 and U^0 nanoparticles with diameters <5 nm as colloidally stable suspensions in tetrahydrofuran (THF) or toluene.

Received: September 28, 2017
Accepted: November 28, 2017
Published: December 21, 2017

© 2017 American Chemical Society

DOI: 10.1021/acsomega.7b01442
ACS Omega 2017, 2, 9144−9149

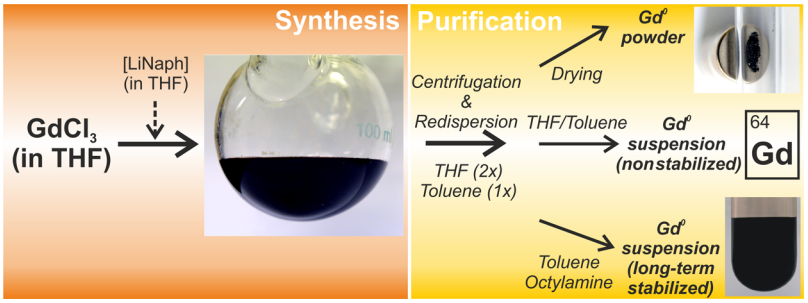

Figure 1. Scheme illustrating the synthesis of Gd^0 nanoparticles including purification and realization of magnetic powder samples as well as of long-term stable octylamine-modified suspensions.

RESULTS AND DISCUSSION

General Aspects. Several requirements are essential for preparing high-quality nanoparticles of highly reactive base metals such as lanthanide and actinide metals. First of all, a powerful reducing agent is essentially required. Here, hydrogen and hydrides (e.g., $[BH_4]^-$ and $[BEt_3H]^-$) as well as elemental metals (e.g., Na^0 and Mg^0) have been suggested.[18] Aiming at metals with a standard electrode potential below −2.0 V, however, hydrides are not powerful enough. Elemental metals, on the other hand, are difficult to handle and need to be dissolved, for instance, in liquid ammonia.[19] Alkaline metal naphthalenides represent an alternative option that was already widely used for establishing main-group element−element bonding,[20,21] as so-called activated Rieke metals in alternative to Grignard reagents in organic synthesis,[22,23] or for obtaining main-group-element nanoparticles such as boron and silicon.[24−26] In view of nanosized transition metals (e.g., Ti^0, Mo^0, W^0, Re^0, Fe^0, and Zn^0), we also have good experience with lithium and sodium naphthalenides ([LiNaph] and [NaNaph]).[27,28]

In fact, [MNaph] (M: Li and Na) is ideal for the synthesis of nanoparticles because the injection of a homogenously dissolved reducing agent is optimal for controlling particle nucleation and particle growth. Hence, the high reducing power causes very fast formation of the elemental metal, which is insoluble in THF. Consequently, high oversaturation occurs, which—in accordance with the model given by LaMer and Dinegar[29]—results in very small particles. Moreover, the deep green [MNaph] solutions are chemically stable for weeks (under argon) and easy to portion with a syringe (in contrast to solid sodium metal), and they can be handled at ambient pressure and temperature (in contrast to liquid ammonia) (Figure 1). Finally, the concentration and the reducing power of the intensely colored [MNaph] solutions can be easily determined via the Lambert−Beer law.

Beside the reducing agent, the use of low-cost metal chlorides (i.e., $GdCl_3$ and UCl_4) as the starting materials and of THF as a standard solvent are specific benefits of the synthesis approach applied here (Figure 1). Thus, elaborate precursors (e.g., carbonyls and organometallic compounds) that need advanced multistep preparation are not needed. All in all, straightforward synthesis of Gd^0 and U^0 nanoparticles as well as of other nanosized lanthanide and actinide metals can be highly relevant in view of their properties, including magnetism (e.g., Sm−Co magnets),[30] catalysis (e.g., Pt_5Ln),[31] superconductivity (e.g., heavy fermion actinide- and lanthanide-based materials),[32] metallic glasses (Ce−Al alloys),[33] or nanodispersed nuclear fuels.[34−36]

Gd^0 Nanoparticles. Gd^0 nanoparticles were made via the [LiNaph]-driven reduction of $GdCl_3$ in THF. The immediate formation of a deep black suspension upon the addition of the greenish [LiNaph] into the colorless $GdCl_3$ solution indicates the formation of Gd^0 nanoparticles (Figure 1). Subsequent to the reaction, side products were removed by repeated centrifugation and redispersion. Thus, LiCl was removed via dissolution in THF; naphthalene was removed by dissolution in toluene (Figure 1). After careful purification, the as-prepared Gd^0 nanoparticles can be either dried in vacuum to obtain blackish powder samples or, in alternative, suspended in THF or toluene to obtain suspensions that are colloidally stable for several hours (i.e., not showing agglomeration and/or sedimentation). For long-term stabilization, a certain amount of octylamine can be added (i.e., 38 mL of toluene with 2 mL of octylamine). Such alkylamines (especially oleylamine) are well-known stabilizers for all kinds of metal nanoparticles.[37] In difference to the literature, however, alkylamines are not required here to control the particle nucleation and only optionally added after the formation of the nanoparticles.

Particle size and particle size distribution of the as-prepared Gd^0 nanoparticles were evaluated by transmission electron microscopy (TEM) (Figure 2). Overview images show uniform nonagglomerated nanoparticles with a narrow size distribution (Figure 2a,b). Statistical evaluation of 100 nanoparticles results in a mean diameter of 2.5 ± 0.7 nm. High-resolution TEM (HRTEM) confirms the uniform spherical shape of the Gd^0 nanoparticles (Figure 2c). Moreover, HRTEM indicates the crystallinity of the as-prepared nanoparticles and clearly shows lattice fringes. Fast Fourier transformation (FFT) analysis of the nanoparticle ensembles confirms an excellent coincidence with the diffraction pattern of hexagonal bulk Gd^0 (lattice parameters: a = 3.62 and c = 5.82 Å) (Figure 2d).[38] Single particles are monocrystalline, as demonstrated by the FFT analysis of a particle on the HRTEM image (Figure 2e), which is also in good agreement with the calculated diffraction pattern of hexagonal bulk Gd^0 (space group: $P6_3/mmc$) in the [210] zone axis (Figure 2f).

Because of the high reactivity of the Gd^0 nanoparticles, not only the chemical synthesis but also the sample handling (e.g., purification procedure, centrifugation, and transfer into the electron microscope) and all analytical characterizations require strict inert conditions and the exclusion of all traces of oxygen and moisture. Thus, the transfer of samples into the electron microscope needs to be performed via suitable vacuum and inert gas transfer modules (see the Supporting Information). Here, it turned out as essential that the resting time of the sample grid with the deposited Gd^0 nanoparticles in the transfer module is as short as possible (<30 min) to avoid oxygen

DOI: 10.1021/acsomega.7b01442
ACS Omega 2017, 2, 9144−9149

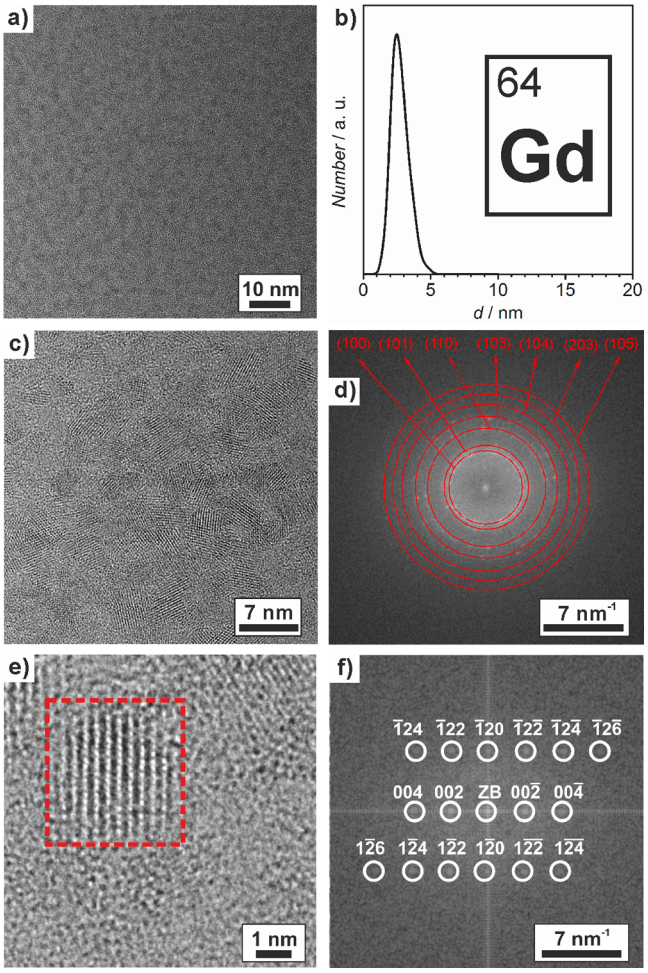

Figure 2. Electron microscopy of the as-prepared Gd^0 nanoparticles: (a) TEM overview image, (b) size distribution based on statistical evaluation of ≥100 nanoparticles on TEM images, (c) HRTEM image, (d) FFT analysis of a particle ensemble, (e) HRTEM image of a single particle, and (f) FFT analysis of the red marked area with calculated diffraction pattern of hexagonal bulk Gd^0 (a = 3.62 and c = 5.82 Å in the [210] zone axis; ZB indicates the zero-order beam).

contamination and formation of Gd_2O_3 (Supporting Information: Figure S1).

The high reactivity of the as-prepared Gd^0 nanoparticles can be demonstrated by two illustrative examples. On the one hand, they even react with the carbon layer of the Lacey carbon copper grid under high-energy-electron bombardment in the electron microscope. On the other hand, octylamine-stabilized nanoparticles that were centrifuged and sintered as powder samples (900 °C) in vacuum, according to X-ray powder diffraction, show reaction to GdN, with octylamine being the only available nitrogen source (Supporting Information: Figure S2). The absence of impurities such as Gd_2O_3, $GdCl_3$, or LiCl, moreover, confirms the purity of the as-prepared nanoparticles.

U^0 Nanoparticles. U^0 nanoparticles were prepared similarly to Gd^0 via [LiNaph]-driven reduction of UCl_4 in THF. Side products of the reaction were again removed by repeated centrifugation in THF (i.e., removal of LiCl) and toluene (i.e., removal of naphthalene). The as-prepared U^0 nanoparticles were either dried to blackish powder samples or redispersed in THF or toluene and result in colloidally highly stable suspensions upon the addition of a certain amount of octylamine. According to TEM analysis, the as-prepared U^0 nanoparticles exhibit a facetted shape and a narrow size distribution with an average particle diameter of 2.0 ± 0.5 nm (Figure 3a,b). The similar size of Gd^0 and U^0 can be attributed

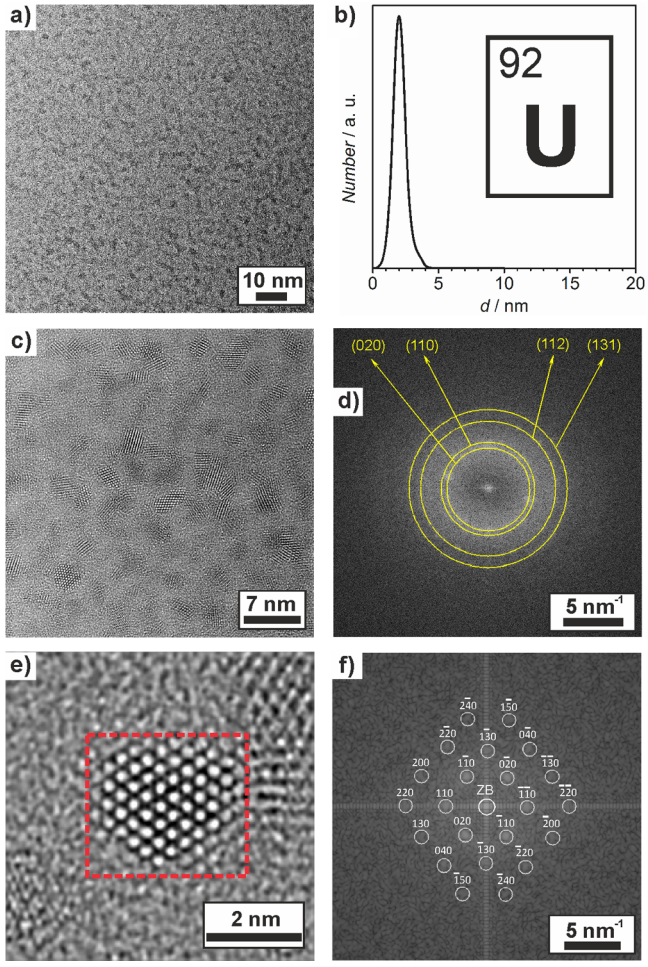

Figure 3. Electron microscopy of the as-prepared U^0 nanoparticles: (a) TEM overview image, (b) size distribution based on statistical evaluation of ≥100 nanoparticles on TEM images, (c) HRTEM image, (d) FFT analysis of a particle ensemble, (e) HRTEM image of a single particle, and (f) FFT analysis of the red marked area with calculated diffraction pattern of orthorhombic bulk α-U^0 (a = 2.85, b = 5.87, and c = 4.96 Å along the [001] zone axis; ZB indicates the zero-order beam).

to the very fast reduction that results in a high supersaturation of insoluble elemental metal in THF. This situation—according to the LaMer model—favors very fast nucleation and the formation of small particles.[29]

The as-prepared U^0 nanoparticles also turned out as crystalline. Thus, HRTEM indicates lattice fringes (Figure 3c,e), and the FFT analysis of the nanoparticle ensembles shows excellent coincidence with the diffraction pattern of orthorhombic bulk α-U^0 (lattice parameters: a = 2.85, b = 5.87, and c = 4.96 Å) (Figure 3d).[39] Single particles are monocrystalline as demonstrated by the good agreement between the FFT of the particle on the HRTEM image (Figure 3e) and the calculated diffraction pattern of bulk orthorhombic α-U^0 (space group: $Cmcm$) in the [001] zone axis (Figure 3f).

To illustrate the high reactivity of the as-prepared U^0 nanoparticles, we have evaluated several reactions. Whereas

DOI: 10.1021/acsomega.7b01442
ACS Omega 2017, 2, 9144−9149

the dark black suspensions of the U^0 nanoparticles in toluene are chemically highly stable under argon, decolorization under the formation of brownish UO_2 suspensions occurred in the presence of air on a timescale of few minutes (Figure 4).

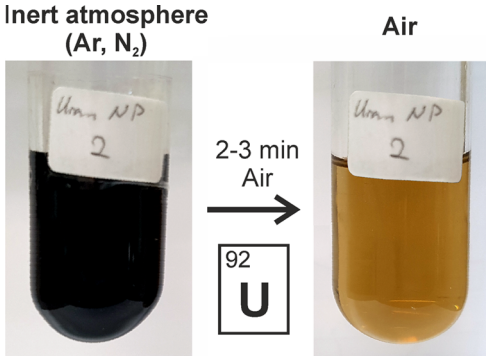

Figure 4. Sensitivity and reactivity of the as-prepared U^0 nanoparticles when in contact with air (2−3 min).

Powder samples of the U^0 nanoparticles react with air, humidity, and acids (e.g., aqueous hydrochloric acid) as well as neat bromine or iodine under immediate ignition. In a more controlled manner, iodine was slowly added to the THF suspensions of the U^0 nanoparticles to form bluish solutions, from which dark blue single crystals were obtained after 2−3 days. Lattice parameter determinations of these single crystals proved their identity as $UI_3 \times 4THF$.[40] This reaction also confirms the reactivity of the as-prepared U^0 nanoparticles.

CONCLUSIONS

Gadolinium (Gd^0) and uranium (U^0) nanoparticles are prepared via lithium naphthalenide ([LiNaph])-driven reduction of $GdCl_3$ and UCl_4, respectively, in THF. Because of the powerful reducing agent, particle nucleation and particle size are well-controlled, which results in uniform nanoparticles with a narrow size distribution with average diameters of 2.5 ± 0.7 nm (Gd^0) and 2.0 ± 0.5 nm (U^0). Specific surface-active agents are not needed to control the particle size. Such a liquid-phase synthesis is shown here for the first time. U^0 nanoparticles are made via the liquid phase for the first time in general. Subsequent to suitable purification, the Gd^0 and U^0 nanoparticles are available as powder samples, suspensions in THF or toluene, or long-term-stabilized suspensions upon the addition of octylamine. The nanoparticles are chemically stable in suspension under inert conditions. However, they are highly reactive in the presence of oxygen and moisture of other oxidizing agents, where they react with immediate ignition.

The straightforward, highly dependable liquid-phase synthesis of Gd^0 and U^0 nanoparticles offers an access to all additional lanthanide and actinide metal nanoparticles. Using THF as the solvent and simple metal chlorides (i.e., $GdCl_3$ and UCl_4) as the starting materials is an additional benefit of the synthesis strategy. Beside fundamental research and establishing a new, reliable liquid-phase synthesis strategy for Gd^0 and U^0, the synthesis of further nanosized lanthanide/actinide metals as well as their use as reactive intermediates for obtaining nanosized lanthanide/actinide compounds (e.g., alloys, intermetallics, sulfides, and nitrides) can become highly relevant. This also includes a bunch of material properties ranging from magnetism, catalysis, and superconductivity to nuclear applications.

EXPERIMENTAL SECTION

Starting Materials. THF (99%, Seulberger) and toluene (99%, Seulberger) were refluxed and freshly distilled from sodium and benzophenone. Octylamine (Aldrich, 99%) was refluxed and distilled in a first step from CaH_2 and thereafter, in a second step, from NaH and degassed by three freeze−pump−thaw cycles. Gadolinium(III) chloride (99.99%, Sigma-Aldrich), lithium (99%, Alfa Aesar), and naphthalene (99%, Alfa Aesar) were used as received. Highly pure single-crystalline uranium(IV) chloride was prepared according to the literature by the chemical transport of UCl_4 prepared in situ from UO_2 and $AlCl_3$.[41]

Lithium naphthalenide ([LiNaph]) was prepared by dissolving 28 mg of Li (4.0 mmol) and 600 mg of naphthalene (4.7 mmol) in 10 mL of THF over a period of 24 h.

Synthesis of Gd^0 Nanoparticles. Gadolinium(III) chloride (703 mg, 2.67 mmol) was dissolved in 20 mL of THF. Thereafter, a solution containing 56 mg of lithium (8.0 mmol) and 1200 mg of naphthalene (9.4 mmol) in 20 mL of THF was added with vigorous stirring. The formation of the Gd^0 nanoparticles can be followed by the naked eye based on the immediate change from a colorless solution to a dark black suspension. The Gd^0 nanoparticles were separated by centrifugation and washed twice by redispersion and centrifugation in/from 20 mL of THF and once in/from toluene. Finally, the nanoparticles were centrifuged and dried in vacuum to obtain powder samples. In alternative, the Gd^0 nanoparticles can be redispersed in 38 mL of THF and 2 mL of octylamine to obtain long-term-stabilized suspensions.

Synthesis of U^0 Nanoparticles. U^0 nanoparticles were prepared similarly to the Gd^0 nanoparticles. Accordingly, 380 mg of UCl_4 (1.0 mmol) was dissolved in 15 mL of THF. Thereafter, a solution containing 28 mg of lithium (4.0 mmol) and 600 mg of naphthalene (4.7 mmol) in 10 mL of THF was injected with vigorous stirring. Again, a deep black suspension was obtained immediately. Separation, washing, and formation of powder samples and suspensions were performed as described above.

Sample Handling. Because of the sensitivity and reactivity of the as-prepared Gd^0 and U^0 nanoparticles, strict sample handling with inert conditions (i.e., Ar and vacuum) is required, ranging from synthesis to sample transfer and all analytical studies (see the Supporting Information).

Safety Advice. Although the as-prepared Gd^0 and U^0 nanoparticles are chemically highly stable in THF or toluene suspensions under inert conditions (Ar), they are highly reactive in the presence of all kinds of oxidizing agents including air, humidity, halogens, and acids. Even alcohols (e.g., hexanol and octanol) lead to heavy evolution of hydrogen. Powder samples are highly pyrophoric and can cause immediate ignition.

Working with radioactive materials may demand special radiation protection depending on your local legislation.

More information regarding the applied analytical techniques can be found in the Supporting Information.

ASSOCIATED CONTENT

Supporting Information

The Supporting Information is available free of charge on the ACS Publications website at DOI: 10.1021/acsomega.7b01442.

Data regarding the analytical techniques, practical handling of the highly reactive base metal nanoparticles

DOI: 10.1021/acsomega.7b01442
ACS Omega 2017, 2, 9144−9149

and their transfer from synthesis to electron microscopy, and thermal behavior and formation of GdN (PDF)

AUTHOR INFORMATION

Corresponding Authors

*E-mail: florian.kraus@chemie.uni-marburg.de. Phone: +49-6421-28-26668. Fax: +49-6421-28-25669 (F.K.).

*E-mail: claus.feldmann@kit.edu. Phone: +49-721-608-42855. Fax: +49-721-608-47021 (C.F.).

ORCID

Claus Feldmann: 0000-0003-2426-9461

Notes

The authors declare no competing financial interest.

ACKNOWLEDGMENTS

C.S., R.P., D.G., and C.F. are grateful to the Deutsche Forschungsgemeinschaft (DFG) for funding of personnel (NanoMet: FE911/11-1, GE 841/29-1) and TEM equipment (INST 121384/33-1 FUGG). Moreover, C.S. acknowledges the Karlsruhe Graduate School of Optics and Photonics (KSOP) for scholarship. F.K. thanks the DFG for his Heisenberg Professorship.

REFERENCES

(1) Ozin, G. A.; Arsenault, A.; Cademartiri, L. *Nanochemistry: A Chemical Approach to Nanomaterials*; RSC Publishing: London, 2005.

(2) Huber, D. L. Synthesis, properties, and applications of iron nanoparticles. *Small* **2005**, *1*, 482−501.

(3) Bard, A. J.; Parsons, R.; Jordan, J. *Standard Potentials in Aqueous Solutions*; Dekker: New York, 1985.

(4) Janiak, C. Metal nanoparticle synthesis in ionic liquids. *Ionic Liquids (ILs) in Organometallic Catalysis*; Topics in Organometallic Chemistry; Springer, 2015; Vol. *51*, pp 17−53.

(5) Zeng, H.; Du, X.-W.; Singh, S. C.; Kulinich, S. A.; Yang, S.; He, J.; Cai, W. Nanomaterials via laser ablation/irradiation in liquid: A Review. *Adv. Funct. Mater.* **2012**, *22*, 1333−1353.

(6) Mariotti, D.; Sankaran, R. M. Microplasmas for nanomaterials synthesis. *J. Phys. D: Appl. Phys.* **2010**, *43*, 323001.

(7) Aruna, I.; Mehta, B. R.; Malhotra, L. K.; Shivaprasad, S. M. Stability and hydrogenation of "bare" gadolinium nanoparticles. *Adv. Funct. Mater.* **2005**, *15*, 131−137.

(8) Nenoff, T. M.; Ferriera, S. R.; Huang, J.; Hanson, D. J. Formation of uranium based nanoparticles via gamma-irradiation. *J. Nucl. Mater.* **2013**, *442*, 162−167.

(9) Trelenberg, T. W.; Glade, S. C.; Tobin, J. G.; Hamza, A. V. The production and oxidation of uranium nanoparticles produced via pulsed laser ablation. *Surf. Sci.* **2006**, *600*, 2338−2348.

(10) Dufort, S.; Le Duc, G.; Salomé, M.; Bentivegna, V.; Sancey, L.; Bräuer-Krisch, E.; Requardt, H.; Lux, F.; Coll, J.-L.; Perriat, P.; Roux, S.; Tillement, O. The high radiosensitizing efficiency of a trace of gadolinium-based nanoparticles in tumors. *Sci. Rep.* **2016**, *6*, 29678.

(11) Detappe, A.; Thomas, E.; Tibbitt, M. W.; Kunjachan, S.; Zavidij, O.; Parnandi, N.; Reznichenko, E.; Lux, F.; Tillement, O.; Berbeco, R. Ultrasmall silica-based bismuth gadolinium nanoparticles for dual magnetic resonance-computed tomography image guided radiation therapy. *Nano Lett.* **2017**, *17*, 1733−1740.

(12) Yang, C.-T.; Padmanabhan, P.; Gulyás, B. Z. Gadolinium(III) based nanoparticles for T_1-weighted magnetic resonance imaging probes. *RSC Adv.* **2016**, *6*, 60945−60966.

(13) Shetty, A. N.; Pautler, R.; Ghaghada, K.; Rendon, D.; Gao, H.; Starosolski, Z.; Bhavane, R.; Patel, C.; Annapragada, A.; Yallampalli, C.; Lee, W. A liposomal Gd contrast agent does not cross the mouse placental barrier. *Sci. Rep.* **2016**, *6*, 27863.

(14) Partridge, S. C.; Kurland, B. F.; Liu, C.-L.; Ho, R. J. Y.; Ruddell, A. Tumor-induced lymph node alterations detected by MRI lymphography using gadolinium nanoparticles. *Sci. Rep.* **2015**, *5*, 15641.

(15) Tsai, K. L.; Dye, J. L. Nanoscale metal particles by homogeneous reduction with alkalides or electrides. *J. Am. Chem. Soc.* **1991**, *113*, 1650−1652.

(16) Nelson, J. A.; Bennett, L. H.; Wagner, M. J. Solution synthesis of gadolinium nanoparticles. *J. Am. Chem. Soc.* **2002**, *124*, 2979−2983.

(17) Yan, C.; Wagner, M. J. Air- and water-stable gold coated gadolinium metal nanocrystals. *Nano Lett.* **2013**, *13*, 2611−2614.

(18) Connelly, N. G.; Geiger, W. E. Chemical redox agents for organometallic chemistry. *Chem. Rev.* **1996**, *96*, 877−910.

(19) Schöttle, C.; Bockstaller, P.; Gerthsen, D.; Feldmann, C. Tungsten nanoparticles from liquid-ammonia-based synthesis. *Chem. Commun.* **2014**, *50*, 4547−4550.

(20) Fischer, R. C.; Power, P. P. π-Bonding and the Lone Pair Effect in Multiple Bonds Involving Heavier Main Group Elements: Developments in the New Millennium. *Chem. Rev.* **2010**, *110*, 3877−3923.

(21) Braunstein, P.; Oro, L. A.; Raithby, P. R. *Metal Clusters in Chemistry*; Wiley-VCH: Weinheim, 2008.

(22) Rieke, R. D. Preparation of organometallic compounds from highly reactive metal powders. *Science* **1989**, *246*, 1260−1264.

(23) Garza-Rodríguez, L. A.; Kharisov, B. I.; Kharisova, O. V. Overview on the synthesis of activated micro- and nanostructurized Rieke metals: history and present state. *Synth. React. Inorg., Met.-Org., Nano-Met. Chem.* **2009**, *39*, 270−290.

(24) Pickering, A. L.; Mitterbauer, C.; Browning, N. D.; Kauzlarich, S. M.; Power, P. P. Room temperature synthesis of surface-functionalized boron nanoparticles. *Chem. Commun.* **2007**, 580−582.

(25) Chiu, H. W.; Chervin, C. N.; Kauzlarich, S. M. Phase changes in Ge nanoparticles. *Chem. Mater.* **2005**, *17*, 4858−4864.

(26) Baldwin, R. K.; Pettigrew, K. A.; Ratai, E.; Augustine, M. P.; Kauzlarich, S. M. Solution reduction synthesis of surface stabilized silicon nanoparticles. *Chem. Commun.* **2002**, 1822−1823.

(27) Schöttle, C.; Bockstaller, P.; Popescu, R.; Gerthsen, D.; Feldmann, C. Sodium-naphthalenide-driven synthesis of base-metal nanoparticles and follow-up reactions. *Angew. Chem., Int. Ed.* **2015**, *54*, 9866−9870.

(28) Schöttle, C.; Doronkin, D. E.; Popescu, R.; Gerthsen, D.; Grunwaldt, J.-D.; Feldmann, C. Ti^0 nanoparticles via lithium-naphthalenide-driven reduction. *Chem. Commun.* **2016**, *52*, 6316−6319.

(29) LaMer, V. K.; Dinegar, R. H. Theory, Production and mechanism of formation of monodispersed hydrosols. *J. Am. Chem. Soc.* **1950**, *72*, 4847−4854.

(30) Frey, N. A.; Peng, S.; Cheng, K.; Sun, S. Magnetic Nanoparticles: synthesis, functionalization, and applications in bioimaging and magnetic energy storage. *Chem. Soc. Rev.* **2009**, *38*, 2532−2542.

(31) Escudero-Escribano, M.; Malacrida, P.; Hansen, M. H.; Vej-Hansen, U. G.; Velazquez-Palenzuela, A.; Tripkovic, V.; Schiotz, J.; Rossmeisl, J.; Stephens, I. E. L.; Chorkendorff, I. Tuning the activity of Pt alloy electrocatalysts by means of the lanthanide contraction. *Science* **2016**, *352*, 73−76.

(32) Aynajian, P.; da Silva, N. E. H.; Gyenis, A.; Baumbach, R. E.; Thompson, J. D.; Fisk, Z.; Bauer, E. D.; Yazdani, A. Visualizing heavy fermions emerging in a quantum critical Kondo lattice. *Nature* **2012**, *486*, 201−206.

(33) Wu, M.; Tse, J. S.; Wang, S. Y.; Wang, C. Z.; Jiang, J. Z. Origin of pressure-induced crystallization of $Ce_{75}Al_{25}$ metallic glass. *Nat. Commun.* **2015**, *6*, 6493.

(34) Hickam, S.; Burns, P. C. Oxo clusters of 5f elements. *Recent Development in Clusters of Rare Earths and Actinides: Chemistry and Materials*; Structure and Bonding; Springer, 2017; Vol. *173*, pp 121−153.

(35) Tyrpekl, V.; Cologna, M.; Vigier, J.-F.; Cambriani, A.; De Weerd, W.; Somers, J. Preparation of bulk-nanostructured UO_2 pellets using high-pressure spark plasma sintering for LWR fuel safety assessment. *J. Am. Ceram. Soc.* **2017**, *100*, 1269−1274.

DOI: 10.1021/acsomega.7b01442
ACS Omega 2017, 2, 9144−9149

(36) Wu, H.; Yang, Y.; Cao, Y. C. Synthesis of colloidal uranium-dioxide nanocrystals. *J. Am. Chem. Soc.* **2006**, *128*, 16522−16523.
(37) Mourdikoudis, S.; Liz-Marzán, L. M. Oleylamine in nanoparticle synthesis. *Chem. Mater.* **2013**, *25*, 1465−1476.
(38) Oudet, X. Comparison between crystal structure and magnetic properties of rare earth and 3d transition metal compounds. *J. Magn. Magn. Mater.* **1985**, *47*−*48*, 397−399.
(39) Eeles, W. T.; Sutton, A. L. X-ray determination of the atomic positions in α-uranium at 22 °C and 600 °C. *Acta Crystallogr.* **1963**, *16*, 575.
(40) Avens, L. R.; Bott, S. G.; Clark, D. L.; Sattelberger, A. P.; Watkin, J. G.; Zwick, B. D. A Convenient Entry into Trivalent actinide chemistry: synthesis and characterization of $AnI_3(THF)_4$ and $An[N(SiMe_3)_2]_3$ (An = U, Np, Pu). *Inorg. Chem.* **1994**, *33*, 2248−2256.
(41) Rudel, S. S.; Kraus, F. Facile syntheses of pure uranium halides: UCl_4, UBr_4 and UI_4. *Dalton Trans.* **2017**, *46*, 5835−5842.

DOI: 10.1021/acsomega.7b01442
ACS Omega 2017, 2, 9144−9149